University of Nebraska - Lincoln
DigitalCommons@University of Nebraska - Lincoln

Anthony F. Starace Publications | Research Papers in Physics and Astronomy

February 1986

Electric-dipole matrix-element formulas in hyperspherical coordinates with applications to H^- and He

Chang-Hwan Park
University of Nebraska - Lincoln

Anthony F. Starace
University of Nebraska-Lincoln, astarace1@unl.edu

Jiang Tan
Kansas State University, Manhattan, Kansas

Chii-Dong Lin
Kansas State University, Manhattan, Kansas

Follow this and additional works at: https://digitalcommons.unl.edu/physicsstarace

Part of the Physics Commons

Park, Chang-Hwan; Starace, Anthony F.; Tan, Jiang; and Lin, Chii-Dong, "Electric-dipole matrix-element formulas in hyperspherical coordinates with applications to H^- and He" (1986). *Anthony F. Starace Publications*. 28.
https://digitalcommons.unl.edu/physicsstarace/28

This Article is brought to you for free and open access by the Research Papers in Physics and Astronomy at DigitalCommons@University of Nebraska - Lincoln. It has been accepted for inclusion in Anthony F. Starace Publications by an authorized administrator of DigitalCommons@University of Nebraska - Lincoln.

Electric-dipole matrix-element formulas in hyperspherical coordinates with applications to H^- and He

Chang-Hwan Park* and Anthony F. Starace
Department of Physics and Astronomy, The University of Nebraska, Lincoln, Nebraska 68588-0111

Jiang Tan and Chii-Dong Lin
Department of Physics, Kansas State University, Manhattan, Kansas 66506
(Received 10 June 1985)

Theoretical formulas for the length, velocity, and acceleration forms of the electric-dipole matrix element within the adiabatic hyperspherical coordinate representation are presented. The length and acceleration formulas are used to calculate the photoionization cross section for He up to 1.0 a.u. above threshold and the photodetachment cross section for H^- up to 0.35 a.u. above threshold. Length- and acceleration-form results for the dipole oscillator strengths for the discrete He transitions, $1sns(^1S^e)\rightarrow 1smp(^1P^o)$, where $n=1$, 2, and 3 and $m=2$, 3, and 4, are also presented. The accuracy of the length- and acceleration-form adiabatic hyperspherical coordinate approximation results is discussed.

I. INTRODUCTION

The first application of the adiabatic hyperspherical approximation[1] to electric-dipole processes was Miller and Starace's calculation[2] of the single photoionization cross section of He (using the length form of the electric-dipole matrix element). It achieved agreement with the experimental measurements of Samson[3] to within 1% at threshold and to within 4% at a photon energy of 1 Ry above threshold. To determine whether such accuracy can be generally expected in hyperspherical coordinate calculations of electric dipole processes, we have undertaken a more extensive theoretical and calculational study. We present here, firstly, theoretical expressions for the length, velocity, and acceleration forms of the electric-dipole matrix element in an adiabatic hyperspherical coordinate representation. We then give the length-and acceleration-form photodetachment cross section for H^- and photoionization cross section for He. Finally, we present the length- and acceleration-form dipole oscillator strengths for the discrete He transitions, $1sns(^1S^e)\rightarrow 1smp(^1P^0)$, where $n=1$, 2, and 3 and $m=2$, 3, and 4. In each case our adiabatic hyperspherical coordinate results are compared with the most accurate results using other calculational methods. Finally, the accuracy of the adiabatic hyperspherical coordinate approximation for electric-dipole processes is assessed.

II. REVIEW OF THE ADIABATIC HYPERSPHERICAL REPRESENTATION

In the hyperspherical coordinate method of Macek,[1] a two-electron wave function $\Psi(\mathbf{r}_1,\mathbf{r}_2)$ is expanded in terms of a complete set of adiabatic eigenfunctions $\Phi_\mu(R,\alpha,\hat{\mathbf{r}}_1,\hat{\mathbf{r}}_2)$, which depend parametrically on the hyperspherical radius $R\equiv(r_1^2+r_2^2)^{1/2}$ and are functions of the five angular variables $\alpha\equiv\tan^{-1}(r_2/r_1)$, $\hat{\mathbf{r}}_1$, and $\hat{\mathbf{r}}_2$. The index μ indicates a particular hyperspherical channel. The form of Ψ is thus

$$\Psi(R,\alpha,\hat{\mathbf{r}}_1,\hat{\mathbf{r}}_2)=(R^{5/2}\sin\alpha\cos\alpha)^{-1}\times\sum_\mu F_\mu(R)\Phi_\mu(R,\alpha,\hat{\mathbf{r}}_1,\hat{\mathbf{r}}_2)\ . \tag{1}$$

The angular or channel function Φ_μ is defined to satisfy the following differential equation in atomic units ($\hbar=e=m=1$):

$$\left[\frac{d^2}{d\alpha^2}-\frac{\mathbf{L}_1^2}{\cos^2\alpha}-\frac{\mathbf{L}_2^2}{\sin^2\alpha}+2R\left[\frac{Z}{\cos\alpha}+\frac{Z}{\sin\alpha}-[1-\sin(2\alpha)\cos\theta_{12}]^{-1/2}\right]\right]\Phi_\mu=U_\mu(R)\Phi_\mu\ . \tag{2}$$

Here $\mathbf{L}_i^2$ is the squared orbital angular momentum operator for the ith electron, $\theta_{12}\equiv\cos^{-1}(\hat{\mathbf{r}}_1\cdot\hat{\mathbf{r}}_2)$, Z is the nuclear charge, and $U_\mu(R)$ is the eigenvalue, which is parametrically dependent on R. Upon substituting Eq. (1) in the two-electron Schrödinger equation and using Eq. (2), one obtains the following set of coupled differential equations for the radial functions $F_\mu(R)$:

$$\left[\frac{d^2}{dR^2}+\frac{U_\mu(R)+\frac{1}{4}}{R^2}+\left[\Phi_\mu,\frac{\partial^2\Phi_\mu}{\partial R^2}\right]+2E\right]F_\mu(R)+\sum_{\mu'\neq\mu}\left[\left[\Phi_\mu,\frac{\partial^2\Phi_{\mu'}}{\partial R^2}\right]+2\left[\Phi_\mu,\frac{\partial\Phi_{\mu'}}{\partial R}\right]\frac{\partial}{\partial R}\right]F_{\mu'}(R)=0\ . \tag{3}$$

 ©1986 The American Physical Society

In Eq. (3) the coupling matrix elements $(\Phi_\mu, \partial^n \Phi_{\mu'}/\partial R^n)$, $n=1,2$, involve integration over the five angular variables only and are thus parametrically dependent on R. Note that the channel functions Φ_μ defined in Eq. (2) are independent of energy E; the energy dependence of the two-electron state in Eq. (1) is carried solely by the radial functions $F_\mu(R)$ defined by Eq. (3).

To solve Eq. (2) we have expanded the channel function Φ_μ in terms of coupled spherical harmonics as follows:

$$\Phi_\mu \equiv \sum_{l_1 l_2} A^{\mu}_{l_1 l_2 LM}(R;\alpha)\mathscr{Y}_{l_1 l_2 LM}(\hat{\mathbf{r}}_1,\hat{\mathbf{r}}_2) , \tag{4a}$$

where

$$\mathscr{Y}_{l_1 l_2 LM}(\hat{\mathbf{r}}_1,\hat{\mathbf{r}}_2) = \sum_{m_1 m_2} Y_{l_1 m_1}(\hat{\mathbf{r}}_1) Y_{l_2 m_2}(\hat{\mathbf{r}}_2)\langle l_1 m_1 l_2 m_2 \mid LM\rangle . \tag{4b}$$

In Eq. (4a) antisymmetry of the wave function is ensured by boundary conditions[1] on the coefficients $A^{\mu}_{l_1 l_2}$. Substituting Eq. (4) in Eq. (2) gives the following differential equation for the expansion coefficients:

$$\left[\frac{d^2}{d\alpha^2} - \frac{l_1(l_1+1)}{\cos^2\alpha} - \frac{l_2(l_2+1)}{\sin^2\alpha} - U_\mu(R)\right] A^{\mu}_{l_1 l_2 LM}(R;\alpha) = -R \sum_{l_1' l_2'} C_{l_1 l_2, l_1' l_2'} A^{\mu}_{l_1' l_2' LM}(R;\alpha) , \tag{5a}$$

where

$$C_{l_1 l_2 l_1' l_2'} \equiv \int_0^{\pi/2} d\alpha \int d\hat{\mathbf{r}}_1 d\hat{\mathbf{r}}_2 \mathscr{Y}^*_{l_1 l_2 LM}(\hat{\mathbf{r}}_1,\hat{\mathbf{r}}_2) C(\alpha,\theta_{12}) \times \mathscr{Y}_{l_1' l_2' LM}(\hat{\mathbf{r}}_1,\hat{\mathbf{r}}_2) , \tag{5b}$$

and

$$C(\alpha,\theta_{12}) \equiv \frac{2Z}{\cos\alpha} + \frac{2Z}{\sin\alpha} - \frac{2}{[1-\sin(2\alpha)\cos\theta_{12}]^{1/2}} . \tag{5c}$$

III. ELECTRIC-DIPOLE MATRIX ELEMENT IN THE ADIABATIC HYPERSPHERICAL REPRESENTATION

Given initial and final two-electron wave functions, Ψ_0 and Ψ_E, of the form of Eq. (1) and using the expansion of the channel functions, Φ_μ, in Eq. (4), one may carry out matrix element angular integrations analytically. We present here our results for the electric-dipole matrix element in the length and acceleration forms[4] in turn. The velocity form,[4] which is not used in our calculations, is presented in the Appendix.

A. Dipole matrix element in the length form

The dipole matrix element for incident light linearly polarized along the z axis in the length form is defined by

$$D_L = \left\langle \Psi_E \left| \hat{\boldsymbol{\epsilon}}_z \cdot \sum_{i=1}^{2} \mathbf{r}_i \right| \Psi_0 \right\rangle \tag{6a}$$

$$= \langle \Psi_E \mid R(\cos\alpha\cos\theta_1 + \sin\alpha\cos\theta_2) \mid \Psi_0 \rangle \tag{6b}$$

$$= \sum_{\mu'\mu} \int_0^\infty dR\, F_{\mu' E}(R) R F_\mu(R) I^L_{\mu'\mu}(R) . \tag{6c}$$

Here $I^L_{\mu'\mu}(R)$ denotes the angular integral, given by

$$I^L_{\mu'\mu}(R) = \sum_{\substack{l_1' l_2' \\ l_1 l_2}} \int_0^{\pi/2} d\alpha\, A^{\mu'}_{l_1' l_2'} \cos\alpha\, A^{\mu}_{l_1 l_2} \sum_{\substack{m_1' m_2' \\ m_1 m_2}} \int d\Omega_1 Y^*_{l_1' m_1'} \cos\theta_1 Y_{l_1 m_1} \int d\Omega_2 Y^*_{l_2' m_2'} Y_{l_2 m_2} \times \langle l_1' m_1' l_2' m_2' \mid L'M'\rangle \langle l_1 m_1 l_2 m_2 \mid LM\rangle$$

$$+ \sum_{\substack{l_1' l_2' \\ l_1 l_2}} \int_0^{\pi/2} d\alpha\, A^{\mu'}_{l_1' l_2'} \sin\alpha\, A^{\mu}_{l_1 l_2} \sum_{\substack{m_1' m_2' \\ m_1 m_2}} \int d\Omega_1 Y^*_{l_1' m_1'} Y_{l_1 m_1} \int d\Omega_2 Y^*_{l_2' m_2'} \cos\theta_2 Y_{l_2 m_2} \times \langle l_1' m_1' l_2' m_2' \mid L'M'\rangle \langle l_1 m_1 l_2 m_2 \mid LM\rangle . \tag{7}$$

Using the orthonormality of spherical harmonics, the following integral over three spherical harmonics,

$$\int d\Omega\, Y_{l'm'}(\Omega)\cos\theta\, Y_{lm}(\Omega) = (-1)^{m'}([l'][l])^{1/2} \begin{pmatrix} l' & 1 & l \\ -m' & 0 & m \end{pmatrix} \begin{pmatrix} l' & 1 & l \\ 0 & 0 & 0 \end{pmatrix} , \tag{8}$$

where $[x] \equiv 2x+1$, and eliminating the sums over m in Eq. (7) by using the summation and transformation formulas for 3-j coefficients, we obtain the following result for $I^L_{\mu'\mu}(R)$:

$$I^L_{\mu'\mu}(R)=\sum_{l_1'l_1l_2}(-1)^{l_2-M'}\begin{Bmatrix}L & L' & 1\\ l_1' & l_1 & l_2\end{Bmatrix}\begin{bmatrix}L & L' & 1\\ -M & M' & 0\end{bmatrix}\begin{bmatrix}l_1' & 1 & l_1\\ 0 & 0 & 0\end{bmatrix}([l_1'][l_1][L'][L])^{1/2}\int_0^{\pi/2}d\alpha\, A^{\mu'}_{l_1'l_2}\cos\alpha\, A^{\mu}_{l_1l_2}$$
$$+\sum_{l_2'l_1l_2}(-1)^{l_1-M'}\begin{Bmatrix}L & 1 & L'\\ l_2' & l_1 & l_2\end{Bmatrix}\begin{bmatrix}L & 1 & L'\\ -M & 0 & M'\end{bmatrix}\begin{bmatrix}l_2' & 1 & l_2\\ 0 & 0 & 0\end{bmatrix}([l_2'][l_2][L'][L])^{1/2}\int_0^{\pi/2}d\alpha\, A^{\mu'}_{l_1'l_2'}\sin\alpha\, A^{\mu}_{l_1l_2}\ . \quad (9)$$

For the special case of the transition ${}^1S\rightarrow{}^1P$ (i.e., $L=0$, $M=0$, and $L'=1$), Eq. (9) reduces to

$$I^L_{\mu'\mu}(R)=\sum_{l_1l_2}3^{-1/2}[l_1]^{-1/2}(l_2||\mathbf{C}^{[1]}||l_1)\times\left[\int_0^{\pi/2}d\alpha\, A^{\mu'}_{l_2l_1}\cos\alpha\, A^{\mu}_{l_1l_1}+\int_0^{\pi/2}d\alpha\, A^{\mu'}_{l_1l_2}\sin\alpha\, A^{\mu}_{l_1l_1}\right], \quad (10a)$$

where

$$(l_2||\mathbf{C}^{[1]}||l_1)\equiv(-1)^{l_2}[l_1]^{1/2}[l_2]^{1/2}\begin{bmatrix}l_2 & 1 & l_1\\ 0 & 0 & 0\end{bmatrix}. \quad (10b)$$

B. Dipole matrix element in acceleration form

The dipole matrix element for incident light linearly polarized along the z axis in the acceleration form is defined by

$$D_A=\left\langle\Psi_E\left|\hat{\epsilon}_z\cdot\sum_{i=1}^{2}\frac{Z\mathbf{r}_i}{r_i^3}\right|\Psi_0\right\rangle \quad (11a)$$

$$=\left\langle\Psi_E\left|\frac{Z}{R^2}\left[\frac{\cos\theta_1}{\cos^2\alpha}+\frac{\cos\theta_2}{\sin^2\alpha}\right]\right|\Psi_0\right\rangle \quad (11b)$$

$$=Z\sum_{\mu'\mu}\int_0^{\infty}dR\, F_{\mu'}R^{-2}F_{\mu E}I^A_{\mu'\mu}\ , \quad (11c)$$

where for the special case of ${}^1S\rightarrow{}^1P$ transitions

$$I^A_{\mu'\mu}=\sum_{l_1l_2}3^{-1/2}[l_1]^{-1/2}(l_2||\mathbf{C}^{[1]}||l_1)\times\left[\int_0^{\pi/2}d\alpha\, A^{\mu'}_{l_2l_1}\cos^{-2}\alpha\, A^{\mu}_{l_1l_1}+\int_0^{\pi/2}d\alpha\, A^{\mu'}_{l_1l_2}\sin^{-2}\alpha\, A^{\mu}_{l_1l_1}\right]. \quad (11d)$$

IV. RESULTS

In this section we present a number of results for electric-dipole transitions from ${}^1S$ states of H^- and He. In calculating our wave functions we make an adiabatic approximation[1] in which we keep only a single term μ in the summation in Eq. (1). For the ground state Ψ_0 this term corresponds to the dominant $1s^2({}^1S)$ configuration; for the final state Ψ_E this term corresponds to the dominant $1s\epsilon p({}^1P)$ configuration. However, this adiabatic approximation is *not* an independent-particle approximation; much correlation is included. For example, in calculating Φ_μ for the initial state, using Eq. (2), an expansion is made in the angular momentum pairs *ss*, *pp*, *dd*, and *ff*; in calculating $\Phi_{\mu'}$ for the final state, an expansion is made in the angular momentum pairs *sp*, *ps*, *pd*, *dp*, *df*, and *fd*. Note that in all our calculations we include the diagonal coupling term when solving Eq. (3) for the radial functions.

The continuum oscillator strength[5] is defined in terms of the length, velocity, and acceleration forms of the electric-dipole matrix element in Eqs. (6), (13), and (15) as follows:

$$\frac{df^L}{dE}=2\omega\,|D_L|^2\ , \quad (12a)$$

$$\frac{df^V}{dE}=\frac{2}{\omega}\,|D_V|^2\ , \quad (12b)$$

$$\frac{df^A}{dE}=\frac{2}{\omega^3}\,|D_A|^2\ , \quad (12c)$$

where ω is the photon energy in atomic units (1 a.u.=27.2108 eV). Note that when discrete final states (denoted by n) are employed in the electric-dipole matrix elements D, Eq. (12) defines the corresponding discrete oscillator strengths f_n^L, f_n^V and f_n^A.

The photoionization or photodetachment cross section, finally, is defined in terms of the continuum oscillator strength as follows:

$$\sigma(\omega)=(2\pi^2/c)df/dE\ . \quad (13)$$

Both Eq. (12) and Eq. (13) assume that the continuum final-state wave function is normalized per unit energy in a.u. Note also that in our calculations for continuum processes we employ Perkeris's values[6] for the binding energies: $I(H^-)=0.027\,751$ and $I(\mathrm{He})=0.903\,72$ a.u.

A. Behavior of $I^L_{\mu'\mu}(R)$ and $I^A_{\mu'\mu}(R)$

As noted in Sec. II, the channel functions Φ_μ are independent of the final-state energy. Hence the angular integrals $I_{\mu'\mu}(R)$ in Sec. III are the same for any photon energy ω or final-state energy E and are characteristic of the initial and final channel functions. In Fig. 1 we show the length- and acceleration-form angular integrals, $I^L_{\mu'\mu}(R)$ [cf. Eqs. (6d) and (10)] and $I^A_{\mu'\mu}(R)$ [cf. Eqs. (11d) and (11e)], for ${}^1S\rightarrow{}^1P$ transitions in H^- and He. Note that these are plotted in Fig. 1 as functions of the scaled radius ZR so that results for both He and H^- could be compared on the same figure. Now asymptotically as $R\cos\alpha(=r_1)\rightarrow\infty$, the channel functions for the lowest ${}^1S$ and ${}^1P$ channels have the following behavior:[1]

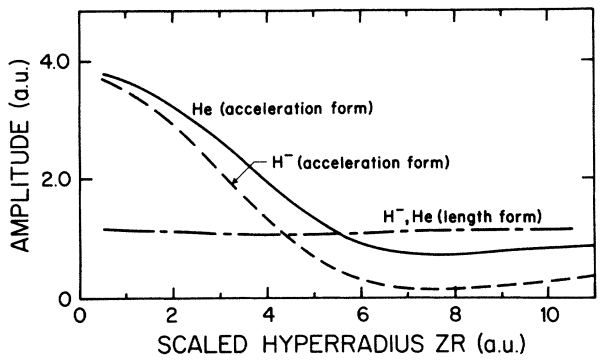

FIG. 1. Length- and acceleration-form angular integrals, $I^L_{\mu'\mu}(R)$ and $I^A_{\mu'\mu}(R)$, for He and H^- plotted vs the scaled radial coordinate ZR.

$$\Phi_\mu(R;\alpha,\hat{\mathbf{r}}_1,\hat{\mathbf{r}}_2)\sim r_1^{1/2}P_{1s}(r_2)Y_{00}(\hat{\mathbf{r}}_2)Y_{l_\mu m_\mu}(\hat{\mathbf{r}}_1)\ , \qquad (14)$$

where $l_\mu=m_\mu=0$ for the ^1S channel and $l_\mu=1$ for the ^1P channel. From Eq. (14), and the relation of the spherical coordinate and hyperspherical coordinate volume elements (i.e., $r_1^2dr_1r_2^2dr_2=R^5\cos^2\alpha\sin^2\alpha\, dR\, d\alpha$) one may show that $I^L_{\mu'\mu}(R)$ approaches a constant as R becomes infinite. This R independence for large R is shown in Fig. 1. Only near the origin is $I^L_{\mu'\mu}(R)$ slightly R dependent as a result of electron correlations. In contrast $I^A_{\mu'\mu}(R)$ is quite R dependent for small R.

B. Discrete energies and dipole oscillator strengths for He

We present adiabatic hyperspherical approximation dipole oscillator strengths for the helium transitions $1sns\ ^1S(n=1,2,3)\rightarrow 1smp\ ^1P(m=2,3,4)$ in Table I. Both our length and acceleration results are presented. The acceleration results, however, are expected to be very unreliable for discrete transitions, particularly for the case $\Delta n=0$, due to the ω^{-3} dependence of f_n^A [cf. Eq. (12c) and the following text]. For this reason we limit our further discussion to our length-form results. They are to be compared in Table I with the accurate variational results of Schiff and Pekeris[7] as well as with some relativistic random-phase-approximation (RRPA) results.[8]

For the transitions $1s^2(^1S^e)\rightarrow 1snp(^1P^0)$ our length results differ from those of Schiff and Pekeris[7] by 5.4% for $n=2$, 2.7% for $n=3$, and 0.0% for $n=4$. By comparison, for $n=2$ the RRPA (Ref. 8) gives an oscillator strength which differs from that of Schiff and Pekeris by -8.8%. For transitions from the $1s2s(^1S^e)$ state to the same final states, our results differ from those of Schiff and Pekeris by -13.3% for $n=2$, $+17.9\%$ for $n=3$, and 14.3% for $n=4$. Finally, for transitions from the $1s3s(^1S^e)$ state to the same final states our results differ from those of Schiff and Pekeris by -10.3% for $n=2$, 0.0% for $n=3$, and $+23.6\%$ for $n=4$. In general, then, our limited number of length-form results indicate a tendency to be larger than those of Schiff and Pekeris[7] and to converge toward their values as n of the final state increases. The exceptions to this are transitions to the same or lower n value, as in those from the excited ^1S states; here our results are lower.

Since the calculated discrete energies are a significant factor in the value of the calculated oscillator strength, especially for the acceleration-form results, we present our adiabatic hyperspherical values for the states involved in Table II. Also shown are experimental[9] values for the level energies. We see that our calculated transition energies differ from the experimental values by less than 2% for transitions from the ground $^1S^e$ state. Calculated transition energies from the two excited $^1S^e$ states, however, are much less reliable because ω itself is smaller, i.e., the initial and final states have much closer energies.

C. Photoionization of He

The length- and acceleration-form results for the photoionization cross section of He are presented in Fig. 2. The velocity-form results were not calculated because of the complexity of the equations in the Appendix. The length results, which are identical to those of Miller and Starace,[2] are 1.2% higher than the experimental measurements of Samson[3] at threshold. The measurements have

TABLE I. Dipole oscillator strengths in helium.

Transition	Present adiabatic hyperspherical results using length (acceleration) form	Variational results[a]	RRPA[b]
$1s^2\,^1S^e\rightarrow$ $1s2p\ ^1P^o$	0.291 (0.342)	0.2762	0.252
$1s3p\ ^1P^o$	0.075 (0.086)	0.073	
$1s4p\ ^1P^o$	0.030 (0.035)	0.030	
$1s2s\ ^1S^e\rightarrow$ $1s2p\ ^1P^o$	0.326 (0.926)	0.376	0.392
$1s3p\ ^1P^o$	0.178 (0.540)	0.151	
$1s4p\ ^1P^o$	0.056 (0.154)	0.049	0
$1s3s\ ^1S^e\rightarrow$ $1s2p\ ^1P^o$	−0.130 (−0.579)	−0.145	
$1s3p\ ^1P^o$	0.539 (21.764)	0.626	
$1s4p\ ^1P^o$	0.178 (0.376)	0.144	

[a]Schiff and Pekeris, Ref. 7.
[b]Lin, Johnson, and Dalgarno, Ref. 8.

TABLE II. Energies for He $^1S^e$ and $^1P^o$ states.

State	Present adiabatic hyperspherical results (a.u.)	Experiment[a] (a.u.)
$1s^2(^1S^e)$	−2.889 125	−2.903 925
$1s2s(^1S^e)$	−2.139 455	−2.175 212
$1s3s(^1S^e)$	−2.059 050	−2.061 265
$1s2p(^1P^o)$	−2.121 460	−2.123 820
$1s3p(^1P^o)$	−2.054 055	−2.055 135
$1s4p(^1P^o)$	−2.030 575	−2.031 065

[a]Reference 9.

error bars of ±3%. This agreement is thus consistent with that for the discrete ^1S and ^1P oscillator strengths from the ground ^1S state presented in Sec. IV B above. The length results equal experiment at 0.1 a.u. above threshold and lie increasingly lower than experiment for higher energies, lying 11.4% lower at 0.9 a.u. above threshold. The acceleration results lie 15.6% higher at threshold and 15.2% lower at 0.9 a.u. above threshold.

Of the many other theoretical calculations, the one with the best overall agreement with the experiment of Samson[3] is also plotted in Fig. 2: the four-channel ($1s$-$2\bar{s}$-$2\bar{p}$) close-coupling calculation of Jacobs.[10] In comparison with the four-channel close-coupling results,[10] the single-channel hyperspherical results in the length form are in better agreement with experiment[3] below $E=0.2$ a.u. and are systematically lower above $E=0.2$ a.u.

D. Photodetachment of H^-

Our length- and acceleration-form adiabatic hyperspherical results for the photodetachment cross section of H^- are presented in Fig. 3. They are compared with the length- and acceleration-form perturbation-variation results of Stewart.[11] Near the peak in the cross section, at

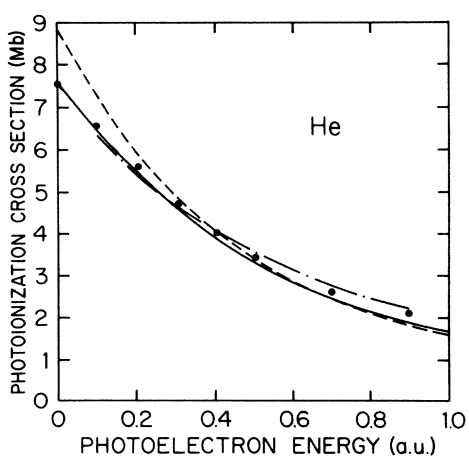

FIG. 2. Photoionization cross section for He, i.e., for $He(^1S^e)+\gamma\rightarrow He^+(1s)(^2S)+e^-$. Present adiabatic hyperspherical coordinate results: solid curve (length form) and dashed curve (acceleration form). Four-channel $1s$-$2\bar{s}$-$2\bar{p}$ close-coupling calculation of Jacobs (Ref. 10): dashed-dotted curve. Experimental measurements of Samson (Ref. 3): solid circles.

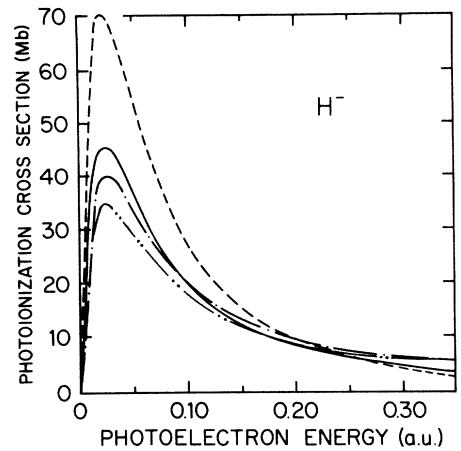

FIG. 3. Photodetachment cross section for H^-, i.e., for $H^-(^1S)+\gamma\rightarrow H(1s)(^2S)+e^-$. Present adiabatic hyperspherical coordinate results: solid curve (length form) and dashed curve (acceleration form). Perturbation-variation results of Stewart (Ref. 11): dash-dotted (length form) and dash—double-dotted (acceleration form).

0.03 a.u. above threshold, our length and acceleration results are, respectively, 12% and 71% higher than the length-form results of Stewart.[11] Above the peak our acceleration results eventually become equal to our length results near 0.275 a.u. They are about 20% lower than the length results of Stewart at this energy. In contrast to our acceleration-form results, Stewart's are lower than his length-form results. As in our calculations, however, Stewart's length and acceleration results tend to converge at higher photon energies.

During the preparation of this manuscript, one of us (A.F.S.) learned that Fink and Zoller[12] have recently also calculated the adiabatic hyperspherical approximation photodetachment cross section for H^- in the length form. Their results agree with ours to within numerical accuracy.

V. DISCUSSION

The high accuracy obtained by Miller and Starace[2] for the photoionization cross section of He using the length form of the electric-dipole matrix element has been found to occur also in the discrete region for electric-dipole transitions from the $^1S^e$ ground state. Length-form results for discrete transitions from excited states or for the photodetachment cross section of H^- have not, however, been found to have comparable accuracy, perhaps due to the greater diffuseness of the initial states and hence the lower reliability of the hyperspherical adiabatic approximation.

In both the photoionization cross section of He and the photodetachment cross section of H^-, the length-form adiabatic hyperspherical approximation results become consistently lower than either experiment or the best alternative theoretical results as the photon energy increases. This has been attributed by Christensen-Dalsgaard[13,14] to inaccuracy of the adiabatic approximation in hyperspherical coordinates at distances far from the nucleus. The acceleration form of the electric-dipole matrix element

weights the region near the nucleus most heavily and thus its use promised to overcome the inadequacy of the adiabatic approximation at large distances. Furthermore, on qualitative grounds the acceleration formula is expected[15] to be accurate at high photon energies, i.e., precisely where the length-form adiabatic hyperspherical results are too low. As shown here, however, the acceleration form gives worse results than the length form near the threshold and gives results approximately equal to those of the length form at high photon energies.

This may be understood from Eq. (11b), which shows that both small R and small α are weighted by the acceleration form. In these regions, in the "valley" of the potential $-C$ [cf. Eq. (5c)], both the ^1S and the ^1P wave functions are relatively inaccurate due to their small amplitudes. In this region the configuration of the system is one in which one electron is near the nucleus and the other one is far away. The correlation effect is thus essentially zero, so that the advantage of hyperspherical wave functions is lost. On the other hand, the small-α and small-R regions are not very important for the length form. Thus we conclude that the results obtained from the acceleration form are less reliable than those of the length form.

It remains of interest, in order to test the accuracy of the adiabatic approximation at large distances, to investigate the velocity-form electric-dipole matrix element, complicated though it may be in hyperspherical coordinates, due to its weighting of intermediate regions of space, where hyperspherical wave functions are well determined. If the velocity-form results give better agreement with experiment than the length-form results this would be added confirmation that the adiabatic approximation breaks down at large radial distances R, the more so as the system energy increases.

ACKNOWLEDGMENTS

This work was supported in part by the U.S. Department of Energy, Office of Basic Energy Sciences, Division of Chemical Sciences, under Contract No. DE-AC02-82ER12081 at Nebraska and Contract No. DE-AC02-76ER10514 at Kansas State.

APPENDIX A: DIPOLE MATRIX ELEMENT IN THE VELOCITY FORM

The dipole matrix element for incident light linearly polarized along the z axis in the velocity form is defined by

$$D_V=\left\langle \Psi_E \left| \hat{\epsilon}_z\cdot\sum_{i=1}^{2}\nabla_i \right| \Psi_0\right\rangle=\left\langle \Psi_E \left| (\cos\alpha\cos\theta_1+\sin\alpha\cos\theta_2)\frac{\partial}{\partial R}+(\sin^2\alpha\cos\theta_1-\cos\alpha\sin\alpha\cos\theta_2)\frac{1}{R}\frac{\partial}{\partial(\cos\alpha)}\right.\right.$$
$$\left.\left.+\frac{\sin^2\theta_1}{R\cos\alpha}\frac{\partial}{\partial(\cos\theta_1)}+\frac{\sin^2\theta_2}{R\sin\alpha}\frac{\partial}{\partial(\cos\theta_2)}\right|\Psi_0\right\rangle . \tag{A1}$$

The four derivative terms in Eq. (A1) act on Ψ_0 as follows:

$$\frac{\partial}{\partial R}\Psi_0=-\tfrac{5}{2}R^{-7/2}(\sin\alpha\cos\alpha)^{-1}F_\mu(R)\sum_{l_1l_2}A^{\mu}_{l_1l_2}(R;\alpha)\mathscr{Y}_{l_1l_2LM}(\hat{\mathbf{r}}_1,\hat{\mathbf{r}}_2)$$
$$+R^{-5/2}(\sin\alpha\cos\alpha)^{-1}F_\mu(R)\sum_{l_1l_2}\frac{\partial A^{\mu}_{l_1l_2}}{\partial R}\mathscr{Y}_{l_1l_2LM}(\hat{\mathbf{r}}_1,\hat{\mathbf{r}}_2)+R^{-5/2}(\sin\alpha\cos\alpha)^{-1}\frac{\partial F_\mu(R)}{\partial R}\sum_{l_1l_2}A^{\mu}_{l_1l_2}\mathscr{Y}_{l_1l_2LM}(\hat{\mathbf{r}}_1,\hat{\mathbf{r}}_2) , \tag{A2a}$$

$$\frac{1}{R}\frac{\partial}{\partial(\cos\alpha)}\Psi_0=R^{-7/2}\left[\frac{1}{\sin^3\alpha}-\frac{1}{\sin\alpha\cos^2\alpha}\right]F_\mu(R)\sum_{l_1l_2}A^{\mu}_{l_1l_2}(R;\alpha)\mathscr{Y}_{l_1l_2LM}(\hat{\mathbf{r}}_1,\hat{\mathbf{r}}_2)$$
$$+R^{-7/2}(-\sin^2\alpha\cos\alpha)^{-1}F_\mu(R)\sum_{l_1l_2}\frac{\partial A^{\mu}_{l_1l_2}}{\partial\alpha}\mathscr{Y}_{l_1l_2LM}(\hat{\mathbf{r}}_1,\hat{\mathbf{r}}_2) , \tag{A2b}$$

$$\frac{\sin^2\theta_1}{R\cos\alpha}\frac{\partial}{\partial(\cos\theta_1)}\Psi_0=R^{-7/2}(\cos^2\alpha\sin\alpha)^{-1}F_\mu(R)$$
$$\times\sum_{l_1l_2}A^{\mu}_{l_1l_2}(R;\alpha)\sum_{m_1m_2}[(l_1+m_1)^{1/2}(l_1-m_1)^{1/2}(2l_1+1)^{1/2}(2l_1-1)^{1/2}$$
$$\times Y_{l_1-1,m_1}(\Omega_1)-l_1\cos\theta_1Y_{l_1m_1}(\Omega_1)]Y_{l_2m_2}(\Omega_2)\langle l_1m_1l_2m_2\,|\,LM\rangle , \tag{A2c}$$

and similarly,

$$\frac{\sin^2\theta_2}{R\sin\alpha}\frac{\partial}{\partial(\cos\theta_2)}\Psi_0=R^{-7/2}(\cos\alpha\sin^2\alpha)^{-1}F_\mu(R)$$
$$\times\sum_{l_1l_2}A^{\mu}_{l_1l_2}(R;\alpha)\sum_{m_1m_2}Y_{l_1m_1}(\Omega_1)[(l_2+m_2)^{1/2}(l_2-m_2)^{1/2}(2l_2+1)^{1/2}(2l_2-1)^{-1/2}$$
$$\times Y_{l_2-1,m_2}(\Omega_2)-l_2\cos\theta_2 Y_{l_2m_2}(\Omega_2)]\langle l_1m_1l_2m_2\,|\,LM\rangle\ . \tag{A2d}$$

Substituting Eq. (A2) into Eq. (A1), we obtain

$$D_V=\left\langle\Psi_E\left|\hat{\epsilon}_z\cdot\sum_{i=1}^{2}\nabla_i\right|\Psi_0\right\rangle$$
$$=\sum_{\mu'\mu}\int_0^\infty dR\left[-\frac{5}{2}\frac{1}{R}\right]F_{\mu'E}F_\mu I^{V,1}_{\mu'\mu}+\sum_{\mu'\mu}\int_0^\infty dR\,F_{\mu'E}F_\mu I^{V,2}_{\mu'\mu}+\sum_{\mu'\mu}\int_0^\infty dR\,F_{\mu'E}\frac{\partial F_\mu}{\partial R}I^{V,3}_{\mu'\mu}$$
$$+\sum_{\mu'\mu}\int_0^\infty dR\,RF_{\mu'E}F_\mu I^{V,4}_{\mu'\mu}+\sum_{\mu'\mu}\int_0^\infty dR(R^{-1})F_{\mu'E}F_\mu I^{V,5}_{\mu'\mu}+\sum_{\mu'\mu}\int_0^\infty dR(R^{-1})F_{\mu'E}F_\mu I^{V,6}_{\mu'\mu}$$
$$+\sum_{\mu'\mu}\int_0^\infty dR(R^{-1})F_{\mu'E}F_\mu I^{V,7}_{\mu'\mu}\ , \tag{A3}$$

where the angular integrals for each of the seven terms above are defined for the special case of ${}^1S\rightarrow{}^1P$ transitions as follows:

$$I^{V,1}_{\mu'\mu}\equiv I^{V,3}_{\mu'\mu}\equiv I^{L}_{\mu'\mu}\ , \tag{A4a}$$

$$I^{V,2}_{\mu'\mu}=\sum_{l_1l_2}3^{-1/2}[l_1]^{-1/2}(l_2||\mathbf{C}^{[1]}||l_1)\left[\int_0^{\pi/2}d\alpha\,A^{\mu'}_{l_2l_1}\cos\alpha\frac{\partial}{\partial R}A^{\mu}_{l_1l_1}+\int_0^{\pi/2}d\alpha\,A^{\mu'}_{l_1l_2}\sin\alpha\frac{\partial}{\partial R}A^{\mu}_{l_1l_1}\right]\ , \tag{A4b}$$

$$I^{V,4}_{\mu'\mu}=\sum_{l_1l_2}3^{-1/2}[l_1]^{-1/2}(l_2||\mathbf{C}^{[1]}||l_1)$$
$$\times\left[\int_0^{\pi/2}d\alpha\,A^{\mu'}_{l_2l_1}[\cos(2\alpha)/\cos\alpha]A^{\mu}_{l_1l_1}-\int_0^{\pi/2}d\alpha\,A^{\mu'}_{l_1l_2}[\cos(2\alpha)/\sin\alpha]A^{\mu}_{l_1l_1}\right]\ , \tag{A4c}$$

$$I^{V,5}_{\mu'\mu}=-\sum_{l_1l_2}3^{-1/2}[l_1]^{-1/2}(l_2||\mathbf{C}^{[1]}||l_1)\left[\int_0^{\pi/2}d\alpha\,A^{\mu'}_{l_2l_1}\sin\alpha\frac{\partial}{\partial\alpha}A^{\mu}_{l_1l_1}-\int_0^{\pi/2}d\alpha\,A^{\mu'}_{l_1l_2}\cos\alpha\frac{\partial}{\partial\alpha}A^{\mu}_{l_1l_1}\right]\ , \tag{A4d}$$

$$I^{V,6}_{\mu'\mu}=-\sum_{l_1l_2}3^{-1/2}l_1[l_1]^{-1/2}(l_2||\mathbf{C}^{[1]}||l_1)\left[\int_0^{\pi/2}d\alpha\,A^{\mu'}_{l_2l_1}(\cos\alpha)^{-1}A^{\mu}_{l_1l_1}+\int_0^{\pi/2}d\alpha\,A^{\mu'}_{l_1l_2}(\sin\alpha)^{-1}A^{\mu}_{l_1l_1}\right]\ , \tag{A4e}$$

and

$$I^{V,7}_{\mu'\mu}=-\sum_{l_1m_1}(-1)^{l_1-m_1}3^{1/2}(l_1+m_1)^{1/2}(l_1-m_1)^{1/2}(2l_1-1)^{-1/2}\begin{bmatrix}l_1-1 & l_1 & 1\\ m_1 & -m_1 & 0\end{bmatrix}$$
$$\times\left[\int_0^{\pi/2}d\alpha\,A^{\mu'}_{(l_1-1)l_1}(\cos\alpha)^{-1}A^{\mu}_{l_1l_1}+\int_0^{\pi/2}d\alpha\,A^{\mu'}_{l_1(l_1-1)}(\sin\alpha)^{-1}A^{\mu}_{l_1l_1}\right]\ . \tag{A4f}$$

Note that $I^{V,6}_{\mu'\mu}$ stems from the second terms in Eqs. (A2c) and (A2d) while $I^{V,7}_{\mu'\mu}$ stems from the first terms of Eqs. (A2c) and (A2d).

---

*Present address: Department of Radiology (Division of Physics), Yale University, 333 Cedar St., New Haven, CT 06510-8040.

[1]J. Macek, J. Phys. B 1, 831 (1968).
[2]D. L. Miller and A. F. Starace, J. Phys. B 13, L525 (1980).
[3]J. A. R. Samson, Phys. Rep. 28, 303 (1976).
[4]A. F. Starace, in *Handbuch der Physik*, edited by W. Mehlhorn (Springer, Berlin, 1982), Vol. 31, pp. 1–121. See Sec. 5.
[5]See Ref. 4, Sec. 8.
[6]C. L. Pekeris, Phys. Rev. 126, 1470 (1962).

[7]B. Schiff and C. L. Pekeris, Phys. Rev. **134**, A638 (1964); B. Schiff, C. L. Pekeris, and Y. Accad, Phys. Rev. A **4**, 885 (1971).
[8]C. D. Lin, W. R. Johnson, and A. Dalgarno, Phys. Rev. A **15**, 154 (1977).
[9]Charlotte E. Moore, *Atomic Energy Levels,* Natl. Bur. Stand. (U.S.) Natl. Stand. Ref. Data Ser. No. 35 (U.S. GPO, Washington, D.C., 1971), Vol. I.
[10]V. L. Jacobs, Phys. Rev. A **3**, 289 (1971).
[11]A. L. Stewart, J. Phys. B **11**, 3851 (1978).
[12]M. Fink and P. Zoller, J. Phys. B **18**, L373 (1985).
[13]B. Christensen-Dalsgaard, Phys. Rev. A **29**, 2242 (1984).
[14]B. Christensen-Dalsgaard (private communication).
[15]A. L. Stewart, Adv. At. Mol. Phys. **3**, 1 (1967).